## PAPER

Check for updates

# Improving the aqueous solubility and antibacterial activity of triclosan using re-dispersible emulsion powder stabilized with gold nanoparticles†

Arathy J. Nair[ab] and Dakrong Pissuwan [iD] *[ab]

Triclosan (TCS) is used as an antibacterial agent in various products. One of the major issues associated with TCS is its limited solubility in aqueous media, which can reduce its effectiveness against bacteria. In this study, we enhanced the aqueous solubility and antibacterial activity of TCS by using a re-dispersible emulsion powder stabilized with gold nanoparticles (GNPs). The developed formulation (TCS/PEG-B/GNPs) demonstrated the ability to dissolve in aqueous media and provided good stability. An antibacterial investigation was conducted using drug-resistant bacterial strains, *Escherichia coli* (*E. coli*) BAA-1161 and methicillin-resistant *Staphylococcus aureus* (MRSA), as model bacteria. The results showed that TCS/PEG-B/GNPs had the highest antibacterial activity. The MRSA strain demonstrated greater susceptibility to TCS (both TCS alone and TCS in the formulation) than *E. coli* BAA-1161. The cytotoxicity assay was also conducted in THP-1 cells and it was found that the viability of THP-1 cells treated with a 5× dilution of TCS/PEG-B/GNPs was higher than 80%. Altogether, our study proposes a novel approach to overcome the solubility concerns of TCS. These results demonstrated an increase in TCS's solubility and efficacy, which holds great promise for future applications.

## 1. Introduction

Over the years, the pharmaceutical industry has grown exponentially. However, the poor aqueous solubility of newly discovered hydrophobic drugs poses an important obstacle at the formulation stage, which restricts their potential applications. Aqueous solubility is a critical factor for the absorption of a drug in the gastrointestinal (GI) lumen.[1] Despite the fact that hydrophobic drugs have a high potential for treating specific diseases, their solubility, administration, and bioavailability restrictions may compromise both their efficacy and safety. Consequently, there is a need to improve formulations to enhance their solubility and bioavailability.

Triclosan (TCS; $C_{12}H_7Cl_3O_2$) is a diphenyl ether with a molecular weight of 289.5 g mol$^{-1}$. It is also known as 5-chloro-2-(2,4-dichlorophenoxy)phenol or 2,4,4′-trichloro-2′-hydroxydiphenyl ether and is widely used in countless personal care products, including antibacterial creams, detergents, soaps, skin cleansers, deodorants, lotions, creams, and toothpastes.[2] It has broad-spectrum antimicrobial activity against both Gram-positive and Gram-negative bacteria, as well as some molds and yeasts. Unfortunately, owing to TCS's poor solubility in aqueous solutions, laboratory experiments using high TCS concentrations under specific conditions are hindered.[3]

An emulsion-forming technique has been used to effectively enhance the bioavailability of hydrophobic drugs that have limited solubility. The droplet size of emulsion droplets can be categorized into three types: nanoemulsion, microemulsion, and macroemulsion droplets. The size of nanoemulsion droplets is commonly in the range of 1–100 nm.[4] Whereas, the droplet size of microemulsion is ~100–400 nm.[4] The macroemulsion droplet size is larger than 400 nm. Using this technique, two major phases, water and oil phases, are prepared. Common systems of emulsion water-in-oil (W/O), oil-in-water (O/W), and complex systems.[5] Surfactants are normally used in emulsion systems as emulsifiers to reduce interfacial tension.[6] In addition, the surfactant molecules surrounding the interfacial site can increase drug stability by shielding the drug from oxidation, hydrolysis, and degradation.[7] However, surfactants easily detach from the interface between oil and water, resulting in emulsion instability.[8] To solve this problem, a lot of researches have shown that the use of nanoparticles into the emulsion system can improve emulsion stability.[8–10] Polyethylene glycol (PEG) is widely used to anchor hydrophobic polymers or hydrophobic drugs.[11–13] It can also act as an emulsifier in single- or double-emulsion systems. PEG, which is located in the water phase, is more involved in the morphology of the emulsion than in the oil phase.[14] In addition to PEG and

*a*Materials Science and Engineering Graduate Program, Faculty of Science, Mahidol University, Bangkok 10400, Thailand. E-mail: dakrong.pis@mahidol.ac.th

*b*Nanobiotechnology and Nanobiomaterials Research (N-BMR) Laboratory, School of Materials Science and Innovation, Faculty of Science, Mahidol University, Bangkok 10400, Thailand

† Electronic supplementary information (ESI) available. See DOI: https://doi.org/10.1039/d4na01022a

nanoparticles, proteins have also been used in emulsions to act as emulsifiers and also increase the stability of emulsion systems.[2]

In this study, we used an emulsion approach to enhance the solubility and bioavailability of TCS. Gold nanoparticles (GNPs) were applied to an emulsion system to increase their stability. GNPs with a size of ~4 nm were applied in the water phase together with PEG and protein (bovine serum albumin, BSA). The oil phase contained TCS. After homogenization and freeze-drying, the resulting formulation, known as TCS/PEG-B/GNPs, was suspended in an aqueous medium. This preparation was then evaluated for its efficacy in eliminating two antibiotic-resistant bacterial strains: *Escherichia coli* (*E. coli*) BAA-1161 and methicillin-resistant *Staphylococcus aureus* (MRSA), in comparison with the original TCS dissolved in an aqueous medium.

Cytotoxicity tests of TCS/PEG-B/GNPs were also performed in blood monocyte THP-1 cells. Our technique here can be useful for enhancing water solubility and bioavailability of poorly water-soluble drugs.[15] The overall work is illustrated in Scheme 1.

## 2. Experimental section

### 2.1. Synthesis of GNPs

The synthesis was modified from the protocol described in previous work published in ref. 16. GNPs with a size of ~4 nm were synthesized by mixing 9.6 mL of a 0.2% gold chloride (HAuCl$_4$) solution with 230.4 mL of Milli-Q water together. The mixture was stirred for 3 min at room temperature. Subsequently, 13.8 mg of trisodium citrate powder (Na$_3$C$_6$H$_5$O$_7$) was added into the already prepared solution of gold chloride. After the tri-sodium citrate was fully dissolved, 5 mL of cold 0.1 M sodium borohydride (NaBH$_4$) dissolved in Milli-Q water was added and continuously stirred for another 8 h. Finally, the color of the mixture transitioned from a pale yellow to a deep orange, which indicated the formation of GNPs. To obtain reproducibility and consistency of experiments, GNPs used in the preparation of all formulations in the next steps were set to have an OD$_{510 nm}$ of 1.0.

### 2.2. Preparation of TCS formulation

An emulsion approach was used to enhance the solubility of TCS in aqueous media. Two distinct phases, comprising a water phase and an oil phase were prepared. The first formulation was prepared by mixing 2 mL of 2% PEG (MW ~ 2000 Da, NOF Co., Ltd, Japan) dissolved in Milli-Q water, 500 μL of 2 mg mL$^{-1}$ BSA (dissolved in Milli-Q water), and 500 μL of Milli-Q water. This mixture was used as the aqueous phase. An oil phase was prepared by dissolving TCS in dichloromethane to obtain TCS at a concentration of 0.5 mg mL$^{-1}$ (w/v). Thereafter, 1 mL of 0.5 mg mL$^{-1}$ TCS was slowly transferred into the water phase.
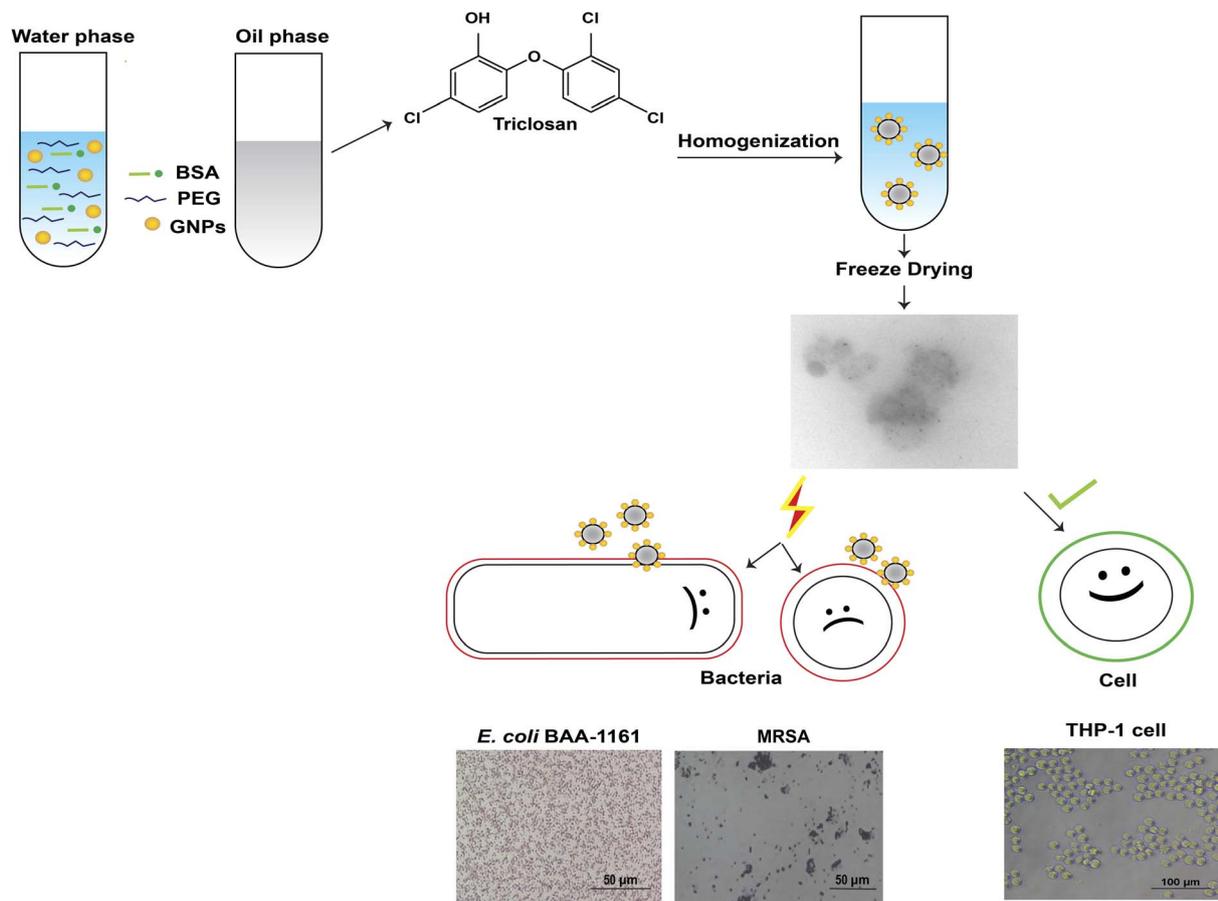


**Scheme 1** Schematic representation of the overall work.

Subsequently, the mixture of both phases was homogenized at 20 500 rpm for 5 min to form the emulsion. After homogenization, the emulsions were frozen in liquid nitrogen for 20 min and lyophilized by freeze-drying for 24 h. This process removed the solvent from the lyophilized sample. The powder of the first formulation obtained after lyophilization is called the TCS/PEG formulation. The second formulation contained 2 mL of 2% PEG, 500 μL of 2 mg mL$^{-1}$ BSA, and 500 μL of 3 nm GNPs as the water phase. The oil phase was the same as that used in the first formulation. The emulsion was homogenized, frozen, and lyophilized to obtain the final powder called TCS/PEG-B/GNPs. The water phases of the third and fourth formulations were prepared in the same manner as those of the first and second formulations, respectively. However, the oil phase contained dichloromethane only. Dichloromethane (1 mL) was gently added to the aqueous phase and homogenized to form an emulsion. After homogenization, the same procedure was performed as described previously. Finally, the obtained powders were named PEG-B and PEG-B/GNPs, respectively. All freeze-dried formulations were dissolved in 3 mL phosphate buffer saline (PBS) before use in further experiments. The developed formulations are listed in Table 1.

Notably, based on the calculation, the concentration of TCS in each formulation was ∼0.17 mg mL$^{-1}$.

## 2.3. Characterization of GNPs and formulations

The light absorption spectra of the GNPs and formulations were measured using a UV-vis spectrophotometer in the range of 400–1000 nm (for GNPs) and 200–1000 nm (for formulations). The size, shape, and distribution of GNPs, as well as the structure of all formulations were investigated using transmission electron microscopy (TEM). The preparation of the samples followed a method consistent with that described in a previous study.[17] The samples were dropped on a copper grid-coated Formvar and then excess liquid was removed using a sharp edge of the filter paper. The samples were stored in a silica gel box until they were ready for TEM observation (JEOL, JEM-1400, Tokyo, Japan). The zeta potential values and polydispersity indices (PDIs) were measured using a Zetasizer dynamic light scattering (DLS) instrument (Malvern Panalytical, Malvern, UK). Energy dispersive X-ray spectroscopy (EDS) equipped with

field emission scanning electron microscope (FESEM) was also used to confirm the presence of GNPs in the formulation.

## 2.4. Investigation of antibacterial activity

In this study, the bacterium *Escherichia coli* (*E. coli*; ATCC BAA-1161) that exhibited resistance to multiple drugs was used as a model bacterium. *E. coli* BAA-1161 bacteria were cultured in nutrient broth (NB) and incubated at 37 °C for 24 h. After incubation, the starting concentration of the bacteria was controlled by adjusting the optical density of the bacterial suspension at 600 nm (OD$_{600\ nm}$) to 0.5. Thereafter, the bacterial suspension was serially diluted in normal saline (0.85% NaCl). Next, the diluted bacterial suspension (500 μL) was mixed with 500 μL of each formulation (TCS/PEG-B, TCS/PEG-B/GNPs, PEG-B, and PEG-B/GNPs). The control sample was prepared by replacing 500 μL of the formulation with PBS. Then, 100 μL of the bacterial suspension from each test was spread on nutrient agar (NA) plates. The plates were incubated at 37 °C for 24 h and the number of bacterial colonies was counted after incubation. The CFU mL$^{-1}$ of bacteria was calculated using the following equation published in ref. 18. MRSA was also prepared using the same process as that used for *E. coli* BAA-1161.

$$\text{CFU mL}^{-1} = \frac{(\text{number of bacteria} \times \text{dilution factor})}{\text{plated volume (mL)}}$$

An investigation of antibacterial activity of original TCS at a concentration of ∼0.17 mg mL$^{-1}$ (dissolved in PBS) was also performed to compare with TCS/PEG-B and TCS/PEG-B/GNPs formulations using the same procedure. The investigation of the antibacterial activity of different concentrations of TCS/PEG-B and TCS/PEG-B/GNPs was also included. Minimum inhibitory concentration (MIC) and minimum bactericidal concentration (MBC) were determined. Additional details are provided in the ESI.†

## 2.5. Investigation on interaction between bacteria and formulation by transmission electron microscope (TEM)

TEM was used to explore the interactions between the bacteria and different formulations. The bacterial suspension was prepared by culturing the bacteria in NB. The bacteria were incubated at 37 °C in a bacterial incubator for 24 h. The bacterial suspension was adjusted to an OD$_{600\ nm}$ of 0.5. The sample was prepared by mixing TCS/PEG-B/GNPs or TCS/PEG-B (500 μL; no dilution and 5× dilution) with 500 μL of bacterial suspension (OD$_{600\ nm}$ = 0.5). After mixing, the samples were centrifuged at 3381 × *g* for 5 min. The supernatant was removed thoroughly and the pellet was dispersed in 500 μL Milli-Q water. Following this, the dispersed solution was centrifuged again under the same condition as mentioned previously. After centrifugation, 10 μL of the resulting pellet was carefully dropped onto a copper grid coated with Formvar. The excess liquid was then removed using filter paper. The grid was then rinsed with 5 μL of Milli-Q water, followed by removal of surplus Milli-Q water with filter paper. The grid was finally dried in a silica gel box for TEM observation.

**Table 1** Summary of sample preparation

| Sample | Water phase | Oil phase (1 mL) |
|---|---|---|
| 1 | 2% PEG 2 mL<br>2 mg mL$^{-1}$ BSA 500 μL<br>Milli-Q water 500 μL | 0.05% TCS in dichloromethane |
| 2 | 2% PEG 2 mL<br>2 mg mL$^{-1}$ BSA 500 μL<br>GNPs 500 μL | 0.05% TCS in dichloromethane |
| 3 | 2% PEG 2 mL<br>2 mg mL$^{-1}$ BSA 500 μL<br>Milli-Q water 500 μL | Dichloromethane |
| 4 | 2% PEG 2 mL<br>2 mg mL$^{-1}$ BSA 500 μL<br>GNPs 500 μL | Dichloromethane |

### 2.6. Determination of cytotoxicity

THP-1 monocytes were cultured in RPMI medium containing 10% fetal bovine serum (FBS) and 1% antibiotics (penicillin–streptomycin). The cells were maintained at 37 °C in a cell incubator and constantly monitored. The cytotoxicity test was slightly modified from that in a previous work.[19] The number of cells was set at $1 \times 10^5$ cells per well (50 μL) in a 96 well plate. To test the formulations, different concentrations of the test samples (TCS/PEG-B and TCS/PEG-B/GNPs) at a volume of 50 μL were added to THP-1 cells. THP-1 cells treated with PBS were used as a control sample in this study. The cells and formulations were incubated for 24 h at 37 °C in a cell incubator. After incubation for 24 h, the CellTiter-Glo assay (Promega, Wisconsin, USA) was used for assessing cell viability, following the manufacturer's protocol. Finally, the luminescence signals of the samples were measured using a microplate reader (TECAN, TECAN Spark™ 10M, Männedorf, Switzerland).

### 2.7. Statistical analysis

The experimental results are expressed as mean values with standard errors. GraphPad Prism software (version 9.0) was used for statistical analysis. To assess statistical significance, ANOVA and Tukey–Kramer tests were applied, with a threshold of $P \leq 0.05$.

## 3. Results and discussion

### 3.1. Characterization of GNPs

The size and morphology of synthesized GNPs were characterized by TEM. As shown in Fig. 1a, the plasmon resonance peak of GNPs was at ~510 nm. The shape of GNPs was spherical with an average size of $4.00 \pm 0.08$ nm (Fig. 1b). The zeta potential value of the GNPs was $-41.80 \pm 0.51$ mV with a PDI value of $0.31 \pm 0.18$ mV. According to our synthetic approach, trisodium citrate was used as a stabilizing agent and sodium borohydride was used as a strong reducing agent;[20] therefore, a negative zeta potential was detected.

### 3.2. Characterization of different TCS formulations

After freeze-drying, all TCS formulations were dissolved in 3 mL PBS before characterization. The absorption spectra of the PEG-B formulation displayed characteristic peaks at ~214 and ~282 nm (Fig. 2a). The maximum light absorption of the first absorption peak is from the peptide backbone conformation[21] and the second weak absorption peak is from the



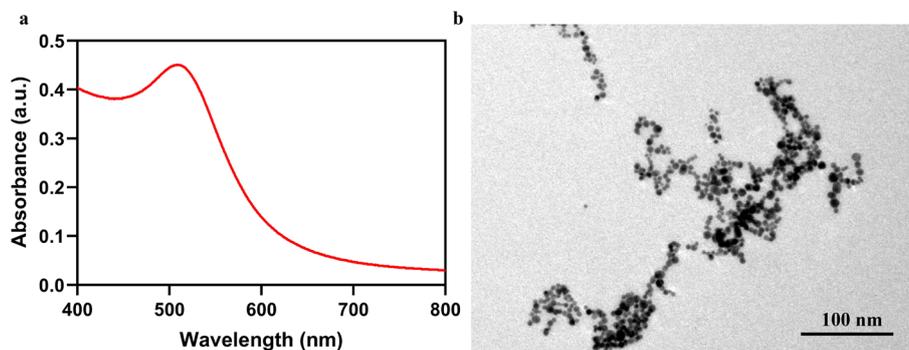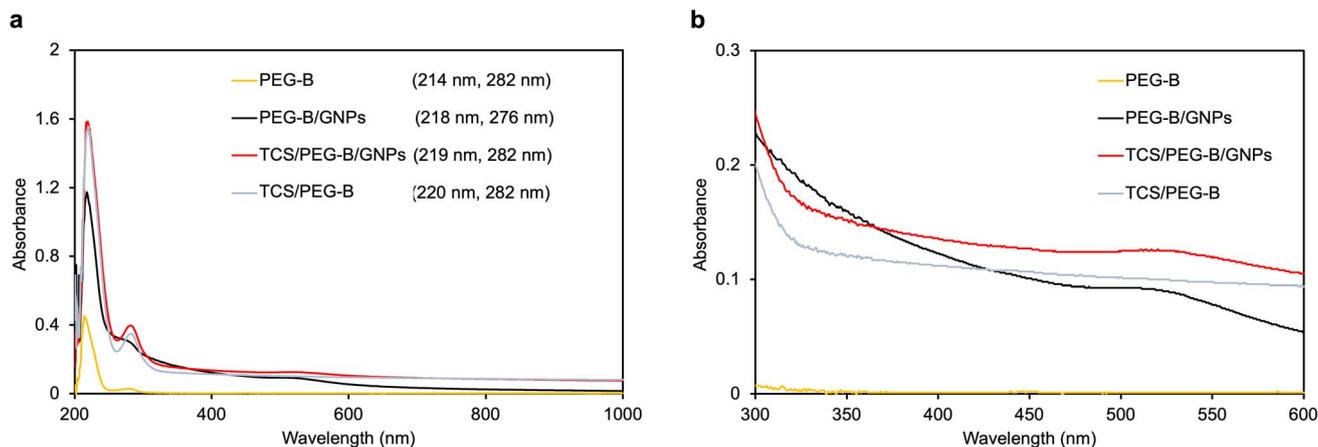Fig. 1 (a) Absorption spectrum of ~4 nm GNPs and (b) TEM image of synthesized GNPs.



Fig. 2 (a) Absorption spectra of PEG-B, PEG-B/GNPs, TCS/PEG-B/GNPs, and TCS/PEG-B and (b) the absorption spectra of the same samples at wavelengths ranging from 300–600 nm. The peaks of GNPs appear in PEG-B/GNPs and TCS/PEG-B/GNPs.
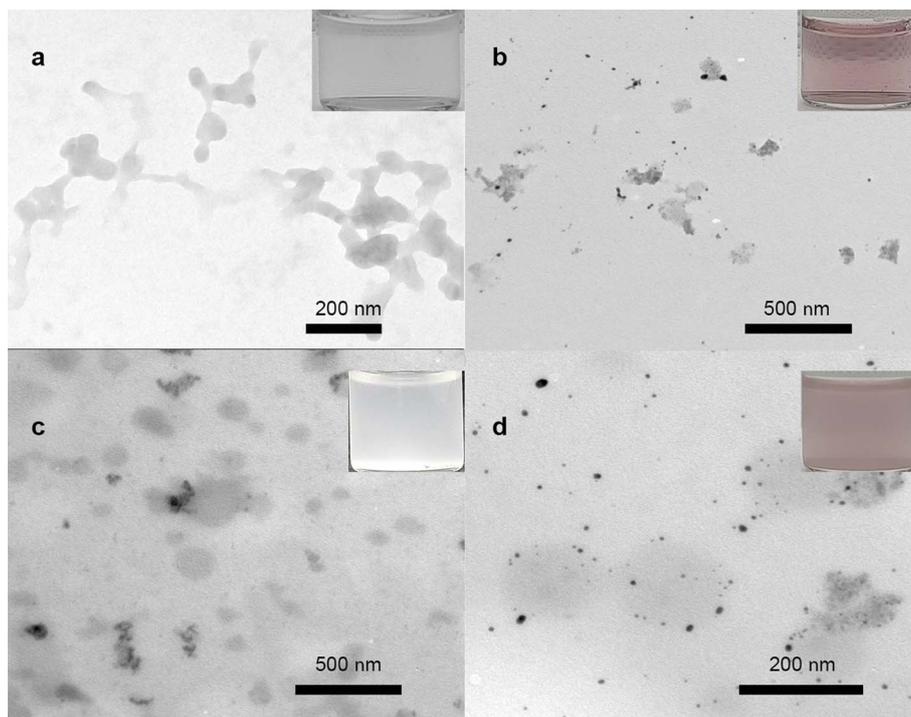
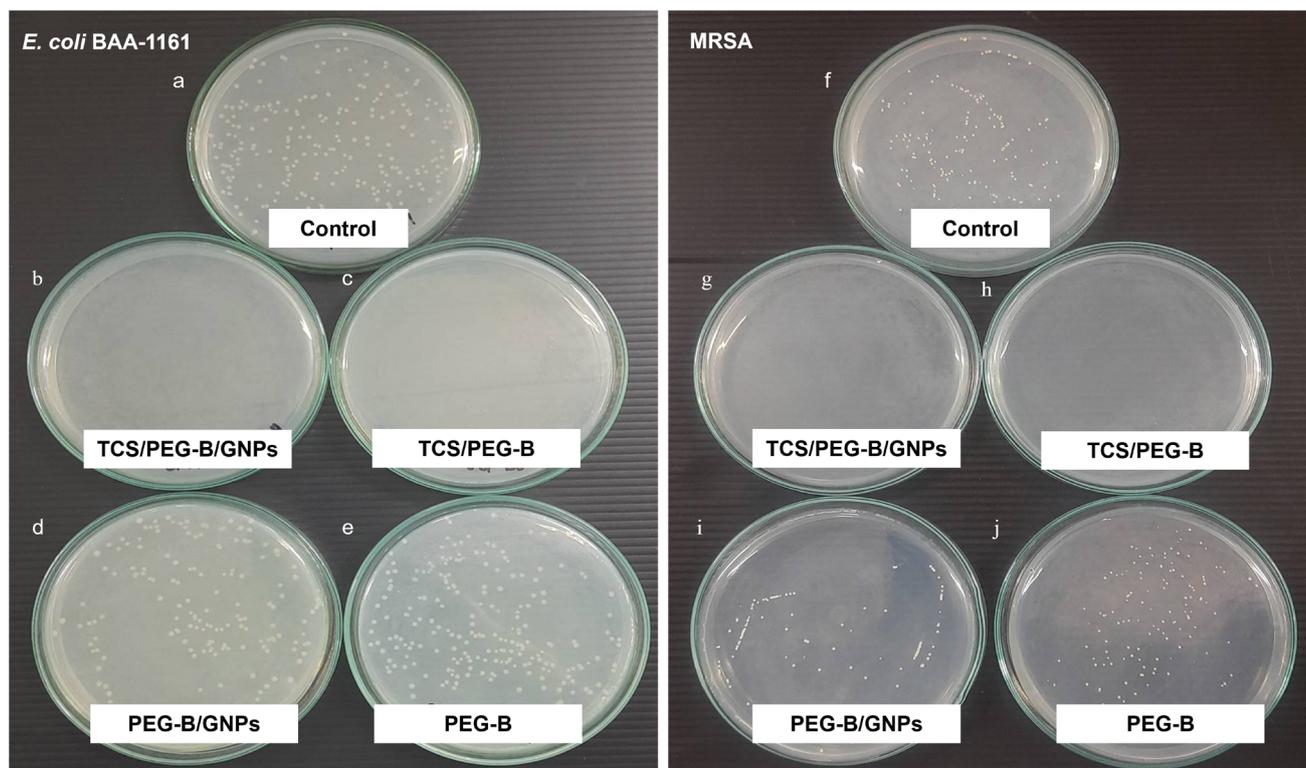**Fig. 3** TEM images of (a) PEG-B, (b) PEG-B/GNPs, (c) TCS/PEG-B, and (d) TCS/PEG-B/GNPs.



**Fig. 4** Images of bacterial colonies of *E. coli* BAA-1161 and MRSA forming on NA. (a and f) Non-treated bacteria, bacteria treated with (b and g) TCS/PEG-B/GNPs, (c and h) TCS/PEG-B, (d and i) PEG-B/GNPs, and (e and j) PEG-B. The concentrations of *E. coli* BAA-1161 and MRSA were ~1.5 × 10³ CFU mL⁻¹ and ~1.7 × 10³ CFU mL⁻¹, respectively.

microenvironment around the aromatic rings of the amino acid of BSA.[22] The first absorption peak of the TCS/PEG-B formulation was red-shifted from 214 nm (PEG-B) to 220 nm (TCS/PEG-B). This red shift indicates an association between TCS and BSA. It was reported that the binding between TCS and BSA could occur through hydrogen bonds between the oxygen atoms of TCS and the amino residues of BSA.[23] Furthermore, a hydrophobic interaction between the benzene rings of TCS and the aromatic side chains of BSA was reported.[24] A second sharp peak at ∼282 nm was detected in the TCS/PEG-B formulation. When GNPs were added to the formulation (TCS/PEG-B/GNPs), the first peak was detected at 219 nm and the second sharp peak at 282 nm was also detected. In contrast, in the absence of TCS, the second peak at 282 nm was very broad and low absorbance was observed for PEG-B. The second peak of the PEG-B/GNPs was observed at ∼276 nm. This could be due to the interaction between GNPs and BSA molecules. It is obvious that the formulations without TCS showed lower absorption in both peaks than those with TCS. Furthermore, their second peaks were broad compared to those of formulations containing TCS. Our findings are similar to those reported by Gu *et al.*[23] Broad absorption peaks of GNPs at ∼520 nm were detected in the PEG-B/GNPs and TCS/PEG-B/GNPs formulations (Fig. 2b). The change in the GNP's absorption peaks observed in the PEG-B/GNPs and TCS/PEG-B/GNPs formulations were attributed to two factors: the refractive index of the surrounding medium present in the formulation and the incorporation of GNPs into these formulations. It has been reported that refractive index of the surrounding environment significantly affects the surface plasmon resonance exhibited by metal nanoparticles.[25] However, this peak was not observed for the PEG-B and TCS/PEG-B formulations. These results indicate that GNPs were associated with the components of the formulations.

The morphologies of all formulations (PEG-B, PEG-B/GNPs, TCS/PEG-B, and TCS/PEG-B/GNPs) were observed using TEM. As expected there was no formation of a structural particle droplet morphology in PEG-B (Fig. 3a). Similar to PEG-B, certain particle droplet morphology did not appear in PEG-B/GNPs. However, GNPs appeared to be randomly distributed in the PEG (Fig. 3b). Non-structured emulsion particles were detected in TCS/PEG-B (Fig. 3c). Spherical oil droplets covered with GNPs were observed in TCS/PEG-B/GNPs (Fig. 3d) after freeze-drying and re-dispersion process in aqueous media (PBS). The similar finding was also reported by Shaheen and Capron.[26] The average size of TCS/PEG-B/GNPs is ∼210.94 ± 14.90 nm.

The formulations prepared in this study were O/W emulsions containing PEG and BSA as the emulsifiers. The BSA was included in the formulation to maintain the emulsion stability. It was reported that the protein is able to facilitate and stabilize the emulsion, especially in polyelectrolyte aqueous media.[27] The GNPs were also added to the formulation because it was reported that the use of nanoparticles in the emulsion system can help increase stability of the emulsion.[28] The GNPs could resist a change of physicochemical properties of the emulsion. After one month, flocculation was observed at the bottom of the bottle containing TCS/PEG-B dispersed in PBS. However, the

flocculation did not appear in TCS/PEG-B/GNPs. This indicates that TCS/PEG-B/GNPs was more stable than TCS/PEG-B.

The zeta potential values of PEG-B, PEG-B/GNPs, TCS/PEG-B, and TCS/PEG-B/GNPs were −16.47 ± 0.99, −16.19 ± 0.45, −17.64 ± 0.28, and −17.69 ± 0.76 mV, respectively. All formulations were negatively charged. The PDI values of PEG-B, PEG-B/GNPs, TCS/PEG-B, and TCS/PEG-B/GNPs were 0.59 ± 0.04, 0.51 ± 0.01, 0.52 ± 0.04, and 0.58 ± 0.01 respectively. The PDI values can reflect the size distribution of particles.[29] It was reported that the PDI values > 0.5 indicate the formation of polydisperse particles.[30] According to TEM images, it revealed that the particles in each formulation had non-uniform sizes.

### 3.3. Bacterial destruction of designed formulations

The initial screening of the effect of PEG-B, PEG-B/GNPs, TCS/PEG-B, and TCS/PEG-B/GNPs on *E. coli* BAA-1161 (∼1.5 × 10³ CFU mL⁻¹) and MRSA destruction (∼1.7 × 10³ CFU mL⁻¹) was performed. It was found that the formulation without TCS had a similar number of bacteria as non-treated bacteria (Fig. 4). In contrast, the formulations containing TCS (TCS/PEG-B and
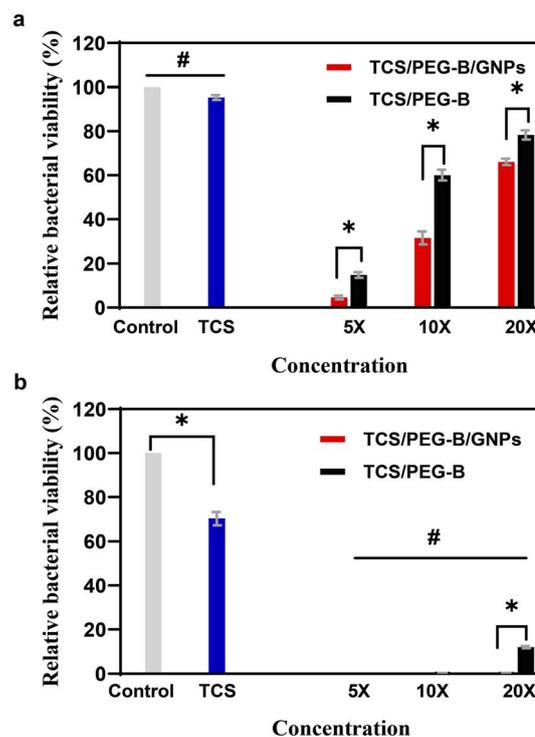


**Fig. 5** Viability of (a) *E. coli* BAA-1161 and (b) MRSA after treatment with TCS/PEG-B and TCS/PEG-B/GNPs at different concentrations and TCS. In (a), * indicates a significant difference in the viability of *E. coli* BAA-1161 between TCS/PEG-B/GNPs and TCS/PEG-B at concentrations of 5×, 10×, and 20× dilutions. # indicates a significant difference in the viability of *E. coli* BAA-1161 compared to *E. coli* BAA-1161 treated with TCS/PEG-B/GNPs and TCS/PEG-B ($p < 0.05$; $n \geq 6$). In (b), * indicates a significant difference in the viability of MRSA between TCS/PEG-B/GNPs and TCS/PEG-B at a concentration of 20× dilution and between control MRSA and MRSA treated with TCS. # indicates a significant difference in the viability of MRSA compared to bacteria treated with TCS/PEG-B/GNPs and TCS/PEG-B ($p < 0.05$; $n \geq 4$).

TCS/PEG-B/GNPs; concentration of TCS in each formulation based on the calculation was ~0.17 mg mL$^{-1}$) were effective in eliminating *E. coli* BAA-1161 and MRSA.

In the next step, we evaluated the viability of *E. coli* BAA-1161 bacteria after exposure to TCS/PEG-B and TCS/PEG-B/GNPs at different concentrations by diluting the original concentrations (containing TCS ~ 0.17 mg mL$^{-1}$) to 5×, 10×, and 20× dilutions. As shown in Fig. 5, the lowest bacterial viability was observed in the 5× dilution of TCS/PEG-B/GNPs (~4.6 ± 0.83%) treatment. The bacterial viability after treating with the 5× dilution of TCS/PEG-B was ~14.88 ± 3.37%. As expected, a higher dilution had a lower effect on *E. coli* BAA-1161 destruction. The viabilities of *E. coli* BAA-1161 bacteria treated with 10× and 20× dilutions of TCS/PEG-B were ~60.10 ± 2.45% and 78.39 ± 2.10%, respectively. In the case of TCS/PEG-B/GNPs, the viabilities of *E. coli* BAA-1161 bacteria were ~31.67 ± 2.88% (for 10× dilution) and ~66.09 ± 1.44% (for 20× dilution). The findings from the studies on antibacterial properties

demonstrated that TCS in the formulations preserved its potent antibacterial capabilities effectively. At the same concentration of TCS, TCS/PEG-B/GNPs were more efficient at destroying *E. coli* BAA-1161 bacteria than TCS/PEG-B (Fig. 5). This indicated that GNPs enhanced the antibacterial activities of TCS in the formulation, which were effective against the drug-resistant bacterial strain *E. coli* BAA-1161. We also investigated the effect of TCS (at the same concentration used in the formulation, ~0.17 mg mL$^{-1}$) dissolved in PBS on *E. coli* BAA-1161 bacterial destruction and found that the viability of bacteria was high (95.36 ± 1.12%, Fig. 5a).

As shown in Fig. 5b, when MRSA bacteria were treated with TCS/PEG-B/GNPs or TCS/PEG-B at 5× dilution, no growth of MRSA bacteria were observed. The MRSA viability of ~0.25 ± 0.12% was observed after treating with TCS/PEG-B at 10× dilution. However, there was no MRSA growth after treating with TCS/PEG-B/GNPs at the same concentration. At 20× dilution, MRSA viabilities after treating with TCS/PEG-B/GNPs and
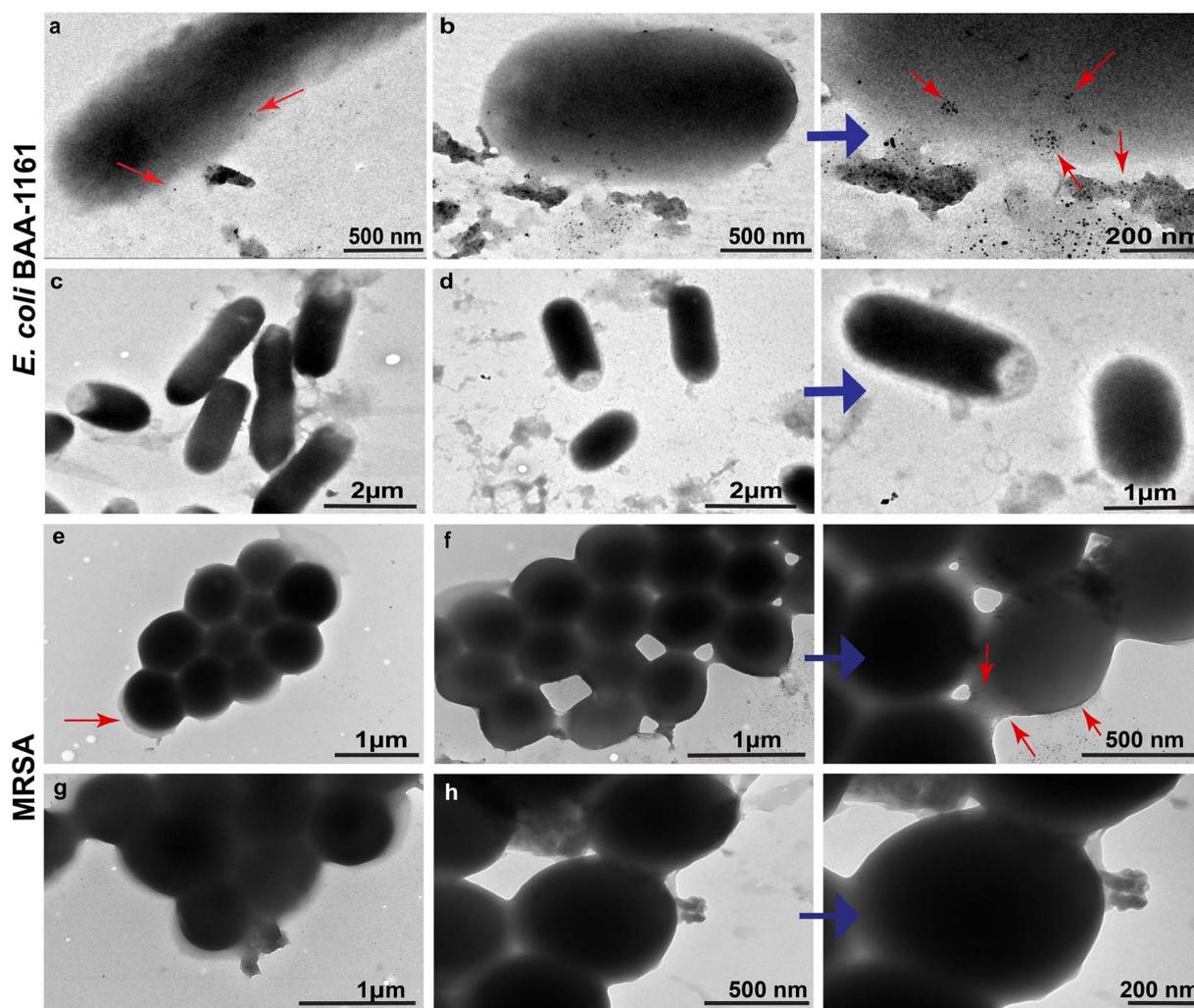


Fig. 6 TEM images of *E. coli* BAA-1161 and MRSA bacteria after treatment with TCS/PEG-B/GNPs at concentrations of (a and e) 5× dilution and (b and f) non-diluted TCS/PEG-B/GNPs, respectively. TEM images of *E. coli* BAA-1161 and MRSA bacteria after treatment with TCS/PEG-B at concentrations of (c and g) 5× dilution and (d and h) non-diluted TCS/PEG-B, respectively. Higher magnification images of *E. coli* BAA-1161 and MRSA bacteria treated with non-diluted TCS/PEG-B/GNPs and TCS/PEG-B are indicated by blue arrows. Spherical black particles appearing in (a, b, e and f) (red arrows) indicate GNPs.

TCS/PEG-B were ~0.21 ± 0.11 and ~11.96 ± 0.48%, respectively. When the same amount of TCS used in the prepared formulations was dissolved in PBS, the MRSA viability was ~70.33 ± 2.41%. Similar to *E. coli* BAA-1161, TCS/PEG-B/GNPs were the most effective at destroying MRSA (Fig. 5). Analysis of TCS- and TCS-containing formulations revealed that MRSA exhibited greater susceptibility to TCS than *E. coli* BAA-1161, when tested against both bacterial strains. The work reported by Huang *et al.*[31] also demonstrated that *S. aureus* was more susceptible to TCS contained in composite scaffolds than *E. coli*. It has been reported that TCS exhibits potent efficacy in combating Gram-positive bacteria.[32] The structural and membrane differences between *E. coli* BAA-1161 and MRSA might influence how TCS- and TCS-based formulations interact with these bacterial strains.

A possible reason for the enhanced bacterial destruction by TCS/PEG-B/GNPs could be a decrease in the diffusion surface area of emulsion droplets,[33] resulting in the slow release of TCS. Consequently, this slow release of TCS could further kill bacteria during the incubation process. According to our findings, preparing a re-dispersible solid (dried TCS/PEG-B/GNPs) in water enhanced the efficiency of TCS in destroying *E. coli* BAA-1161 and MRSA bacteria and the concentration of the

formulation also affected its ability to combat bacteria. The original TCS dissolved in PBS had a low efficiency in destroying both bacterial strains compared to the TCS contained in the designed formulation. This was due to the low solubility of TCS in the aqueous media. Our results strongly confirmed that the designed formulation improved the solubility of TCS. With this formulation, the amount of TCS required to exhibit effective antibacterial activity was also reduced, resulting in a lower risk of overuse of TCS, which can later enhance resistance in further bacterial strains. Furthermore, it can help reduce the amount of TCS distributed in the environment. We also determined the MIC and MBC. The results were in the same direction as those of the plate count agar approach (ESI†).

### 3.4. TEM images of *E. coli* BAA-1161 and MRSA bacteria treated with formulations and energy dispersive X-ray (EDX) spectra of formulations

We investigated the interaction of TCS/PEG-B/GNPs with the bacteria. As shown in Fig. 6a and b, the GNPs were detected around the cell membrane of *E. coli* BAA-1161 bacteria. A lower number of GNPs was detected when a low concentration (5× dilution) of TCS/PEG-B/GNPs was used to treat *E. coli* BAA-1161
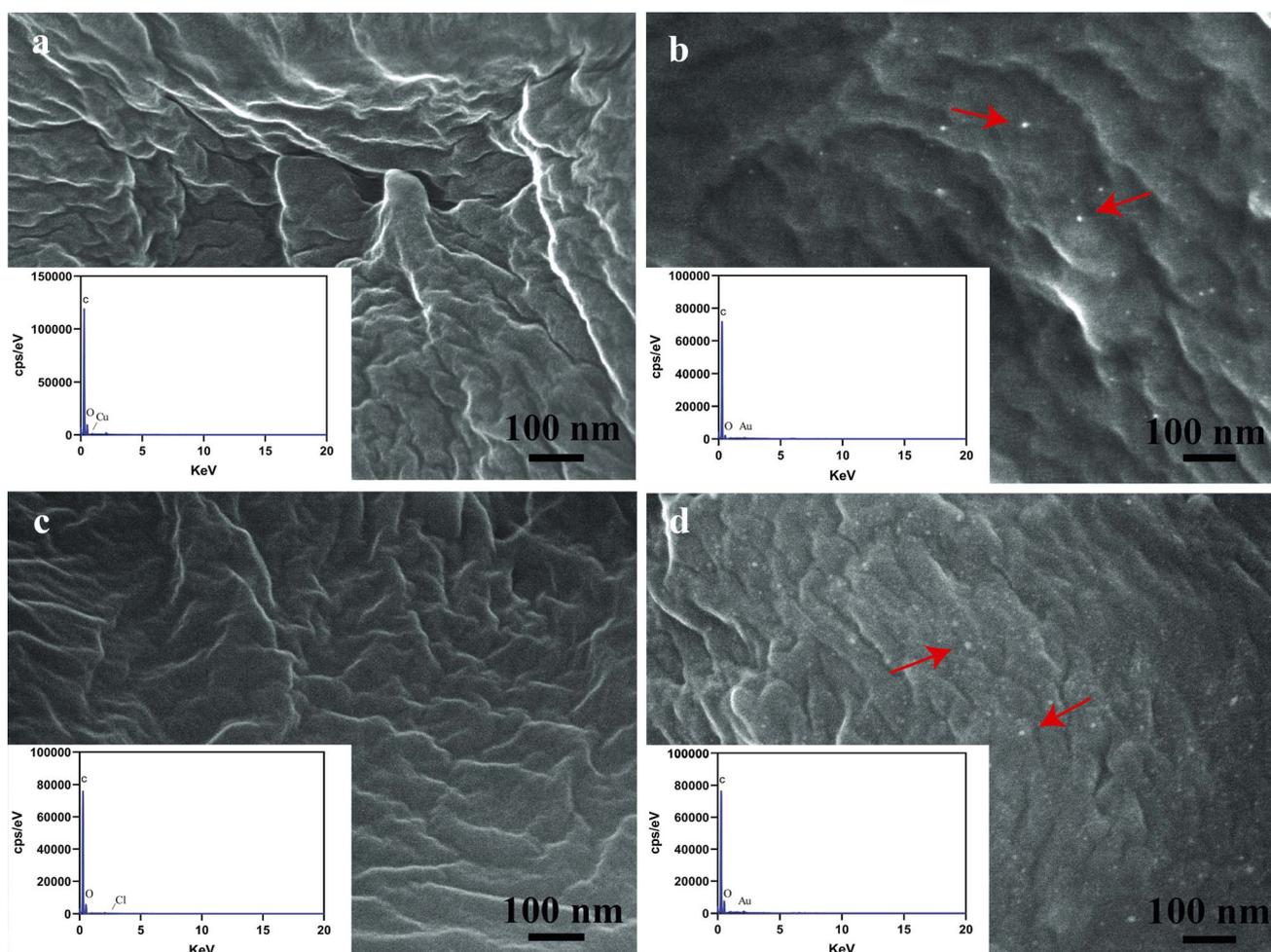


**Fig. 7** SEM images and EDX spectra of (a) PEG-B, (b) PEG-B/GNPs, (c) TCS/PEG-B, and (d) TCS/PEG-B/GNPs.

bacteria (Fig. 6a). In contrast, a greater number of GNPs was observed in *E. coli* BAA-1161 bacteria treated with non-diluted TCS/PEG-B/GNPs (Fig. 6b). As expected, no GNPs were observed in bacteria treated with the 5× dilution (Fig. 6c and g) and non-diluted (Fig. 6d and h) TCS/PEG-B. A higher number of GNPs was also observed in MRSA treated with non-diluted TCS/PEG-B/GNPs (Fig. 6f) than in MRSA treated with 5× dilution TCS/PEG-B/GNPs (Fig. 6e).

According to TEM images, membranes of *E. coli* BAA-1161 and MRSA bacteria treated with TCS/PEG-B and TCS/PEG-B/GNPs were damaged. Upon treating *E. coli* BAA-1161 and MRSA bacteria with TCS/PEG-B/GNPs, it was observed that GNPs were located on the bacterial membranes and were able to penetrate through them. This implies that the interaction between TCS/PEG-B/GNPs and bacteria could enhance bacterial destruction. Additionally, the presence of GNPs at the interface may compromise the stability of the lipid bilayer of the bacterial membrane, potentially resulting in the release of cellular content and subsequent bacterial death. In addition, we verified the inclusion of GNPs in the formulation using EDS. The EDX spectra, as illustrated in Fig. 7b and d, revealed the presence of the gold element exclusively in PEG-B/GNPs (Fig. 7b) and TCS/PEG-B/GNPs (Fig. 7d) formulations. In comparison, the PEG-B and TCS/PEG-B formulations showed no evidence of the gold element in their respective EDX spectra. These findings also substantiate that the spherical particles observed in bacteria treated with TCS/PEG-B/GNPs were certainly GNPs.

### 3.5. Cell viability of THP-1

Because TCS/PEG-B and TCS/PEG-B/GNPs demonstrated high efficiency in the destruction of *E. coli* (BAA-1161) and MRSA, it was worth investigating whether these formulations caused cytotoxicity in mammalian cells. Human monocytic THP-1 cells were used as the model cell in our study. In order to examine the toxicity of our formulation, we focused on the TCS/PEG-B/GNPs and TCS/PEG-B at a concentration of 5× dilution. This concentration was selected because of its ability to destroy *E.*



**Fig. 8** Viability of THP-1 cells treated with undiluted TCS/PEG-B/GNPs and TCS/PEG-B and a 5× dilution of TCS/PEG-B/GNPs and TCS/PEG-B. THP-1 cells without any treatment were used as control cells. * indicates a significant difference in viability of THP-1 cells compared with untreated THP-1 cells (control). ** indicates a significant difference in viability of THP-1 cells between TCS/PEG-B/GNPs and TCS/PEG-B at a 5× dilution ($p < 0.05$; $n \geq 11$).

*coli* BAA-1161 and MRSA. As shown in Fig. 8, the viability of THP-1 cells was $85.65 \pm 1.72\%$ after treating with 5× dilution of TCS/PEG-B/GNPs. As per the guidelines outlined in ISO 10993-5, percentages of cell viability exceeding 80% are generally regarded as non-cytotoxicity.[34] When cells were treated with 5× dilution of TCS/PEG-B, the viability of THP-1 cells was $78.68 \pm 1.25\%$, which was significantly lower than that of TCS/PEG-B/GNPs. This indicates that GNPs not only enhanced antibacterial activity against *E. coli* BAA-1161 and MRSA but also decreased toxicity to THP-1 cells. The toxicity reduction of therapeutic materials prepared using nanoparticles to stabilize emulsion droplets has been reviewed by Wu and Ma.[35] It was reported that the surface roughness of nanoparticles stabilizing at the interface between two immiscible liquids could decrease the uptake of emulsion droplets, ultimately leading to a decrease in toxicity.[36] Non-diluted TCS/PEG-B and TCS/PEG-B/GNPs demonstrated low viabilities of THP-1 cells, which were $13.44 \pm 1.72\%$ and $14.65 \pm 0.25\%$, respectively. Our investigation also focused on the stability of TCS/PEG-B/GNPs and TCS/PEG-B. The PDI can effectively serve as an indicator of particle stability.[29] Specifically, when the PDI value exceeds 0.7, it suggests a significant degree of particle size variation and stability reduction.[37] After PDI measurement, our results demonstrated that after a storage period of 4 weeks, the stability of TCS/PEG-B/GNPs (PDI value = $0.64 \pm 0.06$) was superior to that of TCS/PEG-B (PDI value = $0.88 \pm 0.06$).

## 4. Conclusions

The re-dispersible solid in water emulsion stabilized with GNPs increased the solubility of TCS. The proposed technique here did not use the surfactant; the PEG, BSA, and GNPs were combined together in the aqueous phase. The other phase contained TCS dispersed in dichloromethane. After homogenizing the two phases, freeze drying, and dispersing in PBS, the emulsion droplets were formed (TCS/PEG-B/GNPs) and provided a potent antibacterial property against drug-resistant bacteria, *E. coli* BAA-1161 and MRSA. This confirms that the prepared formulation can accelerate TCS dissolution. The GNPs helped improve the stability of emulsion droplets. Furthermore, the toxicity of TCS was decreased. Further investigation on the effect of shelf life of TCS/PEG-B/GNPs against drug-resistant bacteria and release kinetics that can affect toxicity in healthy cells should be explored in the future. Nevertheless, our investigation provided useful information of a new approach that can be used to prepare TCS as a potent antibacterial agent with low toxicity in various applications.

## Data availability

All experimental data for this study are included in this published article.

## Author contributions

Ms Arathy J. Nair conducted all experiments, contributed to data analysis, methodology, visualization, and prepared the first
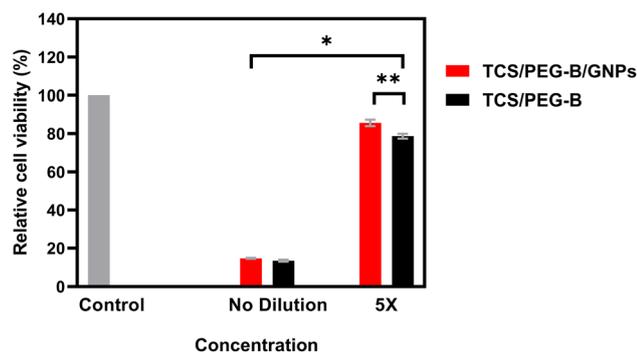
draft of the manuscript, Assoc. Prof. Dakrong Pissuwan contributed to the conceptualization, methodology, visualization, supervision, data analysis, review and editing the entire manuscript, and funding acquisition. All authors approved the final version of the manuscript.

## Conflicts of interest

There are no conflicts to declare.

## Acknowledgements

## References

1 A. Rahman, R. Harwansh, A. Mirza, S. Hussain and A. Hussain, Oral lipid based drug delivery system (LBDDS): formulation, characterization and application: a review, *Curr. Drug Delivery*, 2011, **8**(4), 330–345.

2 M. Zhang, L. Fan, Y. Liu, S. Huang and J. Li, Effects of proteins on emulsion stability: the role of proteins at the oil–water interface, *Food Chem.*, 2022, **397**, 133726.

3 H. P. Schweizer, Triclosan: a widely used biocide and its link to antibiotics, *FEMS Microbiol. Lett.*, 2001, **202**(1), 1–7.

4 E. B. Souto, A. Cano, C. Martins-Gomes, T. E. Coutinho, A. Zielińska and A. M. Silva, Microemulsions and nanoemulsions in skin drug delivery, *Bioengineering*, 2022, **9**, 158.

5 Y. Tian, J. Zhou, C. He, L. He, X. Li and H. Sui, The formation, stabilization and separation of oil-water emulsion: a review, *Processes*, 2022, **10**, 738.

6 D. J. McClements and S. M. Jafari, Improving emulsion formation, stability and performance using mixed emulsifiers: a review, *Adv. Colloid Interface Sci.*, 2018, **251**, 55–79.

7 Y. Jin, D. Liu and J. Hu, Effect of surfactant molecular structure on emulsion stability investigated by interfacial dilatational rheology, *Polymers*, 2021, **13**, 1127.

8 Y.-N. Wu, X. Yan, K. Xu, R.-Y. Wang, M.-J. Cao, X.-D. Wang, Y. Li and C.-L. Dai, Nanoparticle stabilized emulsion with surface solidification for profile control in porous media, *Pet. Sci.*, 2022, **19**, 800–808.

9 G. Kumar, A. Kakati, E. Mani and J. S. Sangwai, Stability of nanoparticle stabilized oil-in-water Pickering emulsion under high pressure and high temperature conditions: comparison with surfactant stabilized oil-in-water emulsion, *J. Dispersion Sci. Technol.*, 2021, **42**, 1204–1217.

10 Z. Briceño-Ahumada, J. F. A. Soltero-Martínez and R. Castillo, Aqueous foams and emulsions stabilized by mixtures of silica nanoparticles and surfactants: a state-of-the-art review, *Chem. Eng. J. Adv.*, 2021, **7**, 100116.

11 D. Chen and M. Jiang, Strategies for Constructing Polymeric Micelles and Hollow Spheres in Solution *via* Specific Intermolecular Interactions, *Acc. Chem. Res.*, 2005, **38**, 494–502.

12 H. T. Oyama, W. T. Tang and C. W. Frank, Effect of hydrophobic interaction in the poly(methacrylic acid)/pyrene end-labeled poly(ethylene glycol) complex, *Macromolecules*, 1987, **20**, 1839–1847.

13 M. S. Webb, D. Saxon, F. M. P. Wong, H. J. Lim, Z. Wang, M. B. Bally, L. S. L. Choi, P. R. Cullis and L. D. Mayer, Comparison of different hydrophobic anchors conjugated to poly(ethylene glycol): effects on the pharmacokinetics of liposomal vincristine, *Biochim. Biophys. Acta, Biomembr.*, 1998, **1372**, 272–282.

14 Z. Wang, J. Song, S. Zhang, X.-Q. Xu and Y. Wang, Formulating polyethylene glycol as supramolecular emulsifiers for one-step double emulsions, *Langmuir*, 2017, **33**, 9160–9169.

15 M. Karimi, S. Bahrami, S. B. Ravari, P. S. Zangabad, H. Mirshekari, M. Bozorgomid, S. Shahreza, M. Sori and M. R. Hamblin, Albumin nanostructures as advanced drug delivery systems, *Expert Opin. Drug Delivery*, 2016, **13**, 1609–1623.

16 C. Deraedt, L. Salmon, S. Gatard, R. Ciganda, R. Hernandez, J. Ruiz and D. Astruc, Sodium borohydride stabilizes very active gold nanoparticle catalysts, *Chem. Commun.*, 2014, **50**, 14194–14196.

17 D. Pissuwan, K. Nose, R. Kurihara, K. Kaneko, Y. Tahara, N. Kamiya, M. Goto, Y. Katayama and T. Niidome, A solid-in-oil dispersion of gold nanorods can enhance transdermal protein delivery and skin vaccination, *Small*, 2011, **7**, 215–220.

18 P. Amornwairat and D. Pissuwan, Colorimetric sensing of Gram-negative and Gram-positive bacteria using 4-mercaptophenylboronic acid-functionalized gold nanoparticles in the presence of polyethylene glycol, *ACS Omega*, 2023, **8**, 13456–13464.

19 S. Chaicherd, M. C. Killingsworth and D. Pissuwan, Toxicity of gold nanoparticles in a commercial dietary supplement drink on connective tissue fibroblast cells, *SN Appl. Sci.*, 2019, **1**, 336.

20 R. Seoudi and F. Al-Marhaby, Synthesis, characterization and photocatalytic application of different sizes of gold nanoparticles on 4-nitrophenol, *World J. Nano Sci. Eng.*, 2016, **6**, 120–128.

21 L. Zhao, Y. Zhao, H. Teng, S. Shi and B. Ren, Spectroscopic investigation on the interaction of titanate nanotubes with bovine serum albumin, *J. Appl. Spectrosc.*, 2014, **81**, 719–724.

22 S.-T. Duan, B.-S. Liu, T.-T. Li and M.-M. Cui, Study of the interaction of cefonicid sodium with bovine serum albumin by fluorescence spectroscopy, *J. Appl. Spectrosc.*, 2017, **84**, 431–438.

23 J. Gu, S. Zheng, H. Zhao and T. Sun, Investigation on the interaction between triclosan and bovine serum albumin by spectroscopic methods, *J. Environ. Sci. Health, Part B*, 2020, **55**, 52–59.

24 J. Chen, X. Zhou, Y. Zhang, Y. Zi, Y. Qian, H. Gao and S. Lin, Binding of triclosan to human serum albumin: insight into the molecular toxicity of emerging contaminant, *Environ. Sci. Pollut. Res. Int.*, 2012, **19**, 2528–2536.

25 C. Novo, A. M. Funston, S. I. Pastoriza, L. M. Liz-Marzan and P. Mulvaney, Influence of the medium refractive index on the optical properties of single gold triangular prisms on a substrate, *J. Phys. Chem. C*, 2018, **112**, 3–7.

26 T. I. Shaheen and I. Capron, Formulation of re-dispersible dry o/w emulsions using cellulose nanocrystals decorated with metal/metal oxide nanoparticles, *RSC Adv.*, 2021, **11**, 32143–32151.

27 M. Saito, L.-J. Yin, I. Kobayashi and M. Nakajima, Comparison of stability of bovine serum albumin-stabilized emulsions prepared by microchannel emulsification and homogenization, *Food Hydrocolloids*, 2006, **20**, 1020–1028.

28 D. Arab, A. Kantzas and S. L. Bryant, Nanoparticle stabilized oil in water emulsions: A critical review, *J. Pet. Sci. Eng.*, 2018, **163**, 217–242.

29 M. J. Masarudin, S. M. Cutts, B. J. Evison, D. R. Phillips and P. J. Pigram, Factors determining the stability, size distribution, and cellular accumulation of small, monodisperse chitosan nanoparticles as candidate vectors for anticancer drug delivery: application to the passive encapsulation of [14C]-doxorubicin, *Nanotechnol., Sci. Appl.*, 2015, 67–80.

30 A. B. Darwish, A. M. Mohsen, S. ElShebiney, R. Elgohary and M. M. Younis, Development of chitosan lipid nanoparticles to alleviate the pharmacological activity of piperine in the management of cognitive deficit in diabetic rats, *Sci. Rep.*, 2024, **14**, 8247.

31 R. Huang, M. Hu, W. Liang, J. Zheng, Y. Du, Y. Lin, H. Wang, W. Guo, Z. Zeng, C. Li, M. Li, H. Wang and X. Zhang, One-step preparation of green fabric for continuous antibacterial applications, *Engineering*, 2021, **7**, 326–333.

32 Coming clean, *Nat. Chem. Biol.*, 2005, vol. 1, p. 349, https://www.nature.com/articles/nchembio1205-349.

33 J. Li, X. Xu, Z. Chen, T. Wang, Z. Lu, W. Hu and L. Wang, Zein/gum Arabic nanoparticle-stabilized Pickering emulsion with thymol as an antibacterial delivery system, *Carbohydr. Polym.*, 2018, **200**, 416–426.

34 ISO 10993-5, *Biological Evaluation of Medical Devices—Part 5: Tests for In Vitro Cytotoxicity*, International Organization for Standardization, Geneva, 2009, p. 34.

35 J. Wu and G. H. Ma, Recent studies of Pickering emulsions: particles make the difference, *Small*, 2016, **12**, 4633–4648.

36 A. Schrade, V. Mailänder, S. Ritz, K. Landfester and U. Ziener, Surface roughness and charge influence the uptake of nanoparticles: fluorescently labeled pickering-type *versus* surfactant-stabilized nanoparticles, *Macromol. Biosci.*, 2012, **12**, 1459–1471.

37 M. Danaei, M. Dehghankhold, S. Ataei, D. F. Hasanzadeh, R. Javanmard, A. Dokhani, S. Khorasani and M. R. Mozafari, Impact of particle Size and Polydispersity Index on the Clinical Applications of Lipidic Nanocarrier Systems, *Pharmaceutics*, 2018, **10**, 57.